

Stable Mesoscopic Dye-Sensitized Solar Cells Based on Tetracyanoborate Ionic Liquid Electrolyte

Daibin Kuang, Peng Wang,[†] Seigo Ito, Shaik. M. Zakeeruddin,* and Michael Grätzel*

Laboratory for Photonics and Interfaces, Institute of Chemical Sciences and Engineering,
Ecole Polytechnique Fédérale de Lausanne, 1015 Lausanne, Switzerland

Received March 12, 2006; E-mail: shaik.zakeer@epfl.ch; michael.graetzel@epfl.ch

Mesoscopic dye-sensitized solar cells (DSC)¹ have attracted considerable attention in the last 15 years as a potential alternative to conventional inorganic photovoltaics.¹ Significant progress has been made in the development of efficient dyes, electrolytes, and nanocrystalline metal oxide films for the enhancement of the device performance.^{2–4} Encapsulation of volatile organic electrolytes with high vapor pressure is a major challenge in practical applications of the DSC. Room temperature ionic liquids (ILs) are attractive candidates for replacement of the volatile organic solvents due to their negligible vapor pressure and high ionic conductivity.^{5–7} Unfortunately, pure imidazolium iodide/triiodide ILs are very viscous, and the high concentration of iodide ions in the electrolyte creates a loss channel through reductive quenching of the excited sensitizer, hampering device performance.^{7d} The use of some binary ionic liquid electrolytes in DSC allows the reduction of electrolyte viscosity and avoids efficiency losses.^{7b–e} However, thermal instability under prolonged testing at 80 °C for DSC devices based on these system is normally observed.

The search for new highly conductive ILs containing thermally and chemically robust anions is, therefore, of great importance. Tetracyanoborate is very attractive in this respect and was first reported by Bernhardt et al.⁸ The negative charge is uniformly delocalized over the four cyano groups tetrahedrally surrounding the boron cation. 1-Ethyl-3-methylimidazolium tetracyanoborate (EMIB(CN)₄) is a new ionic liquid (Figure S1) of a low viscosity (19.8 cP at 20 °C) and high chemical and thermal stability.⁹ DSC investigated below employed a binary ionic liquid composed of 0.2 M I₂, 0.5 M *N*-methylbenzimidazole, and 0.1 M guanidinium thiocyanate in a mixture of 1-propyl-3-methylimidazolium iodide (PMII) and EMIB(CN)₄ (volume ratio, 13:7), in combination with the amphiphilic sensitizer (Z-907Na). The conductivity of the electrolyte was measured as 4.77 mS cm⁻¹ at 30 °C. The apparent diffusion coefficients of iodide and triiodide were derived as 4.08 × 10⁻⁷ and 3.42 × 10⁻⁷ cm² s⁻¹, respectively, from the anodic and cathodic steady-state currents (*I*_{ss}) measured by a microelectrode (Figure S2), using the equation $I_{ss} = 4ncaFD_{app}$.¹⁰

The photoanodes of the DSC employed in the experiments were composed of a 6.8 μm thick transparent TiO₂ layer (20 nm sized particles) and with a scattering layer (TiO₂, 400 nm sized particles) of 4 μm thickness. The electrode was dipped into 300 μM Z-907Na dye solution in a mixture of acetonitrile and *tert*-butyl alcohol (volume ratio, 1:1) at room temperature for 14 h to afford sensitization. The double layer structured mesoscopic TiO₂ film preparation and the DSC device fabrication were carried out as reported earlier.^{7e} Figure 1 illustrates the photocurrent density–voltage curves. The short-circuit photocurrent density (*J*_{sc}), open-circuit photovoltage (*V*_{oc}), and fill factor (FF) of the device A with Z-907Na alone are 12.7 mA cm⁻², 716 mV, and 0.704, respectively, yielding a photovoltaic conversion efficiency of 6.4%. In the

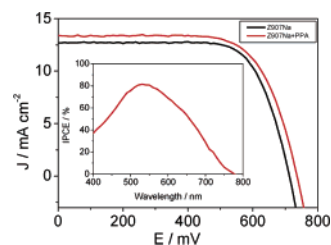


Figure 1. Current density–voltage characteristic of DSC devices under AM 1.5 simulated full sunlight (100 mW cm⁻²) illumination. The inset shows the incident photon-to-current conversion efficiency plotted as a function of wavelength of the exciting light. Cell active area = 0.158 cm².

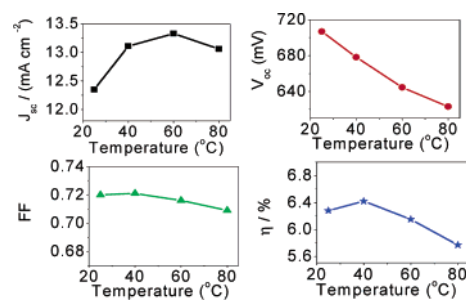


Figure 2. Effect of temperature on the DSC's photovoltaic performance.

presence of 3-phenylpropionic acid (PPA) as coadsorbent (device B), the corresponding photovoltaic parameters (*J*_{sc}, *V*_{oc}, FF, η) are 13.55 mA cm⁻², 736 mV, 0.698, and 7.0, respectively. At the lower light irradiances of 53 and 30 mW cm⁻², the efficiencies are 7.4 and 7.7%, respectively. The photocurrent action spectrum of device B (inset of Figure 1) shows that the incident photon-to-current conversion efficiency (IPCE) reaches 80% at 530 nm.

The influence of operating temperature on the photovoltaic parameters of the DSC was investigated in the range of 25–80 °C. Photovoltaic performance parameters (*J*_{sc}, *V*_{oc}, FF, and η) of devices measured at 25, 40, 60, and 80 °C under 1 sun illumination are shown in Figure 2 with the current–voltage characteristics illustrated in Figure S3. The short-circuit photocurrent increases with temperature up to 60 °C mainly due to the decrease in the viscosity of the electrolyte, facilitating the mass transport of triiodide ions as evidenced by the photocurrent transient measurements shown in Figure S4. Photocurrent may also be gained by thermally activating electron injection from occupied sensitizer states that are located near or slightly below the thermodynamic threshold. Between 60 and 80 °C, the photocurrent decreases once again probably due to enhanced recapture of electrons by triiodide resulting in lower electron collection efficiency. Following the same reasoning, the dark current increases with temperature, resulting in a decrease of the open circuit photovoltage as shown in Figure S3. The temperature effect on the fill factor remained small in the investigated domain.

[†] Present address: Cavendish Laboratory, Madingley Road, Cambridge, CB3 0HE, U.K.

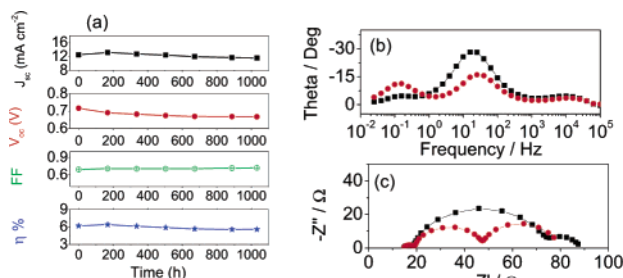


Figure 3. (a) Evolution of photovoltaic parameter (AM 1.5 full sunlight) of device during continued thermal aging at 80 °C in the dark. (b) Bode phase plots and (c) Nyquist plots of the device for fresh (black) and aging cells (red) at 80 °C for 1000 h, measured at -0.7 V bias in dark.

The negligible temperature effect in the 25–60 °C range on the overall photovoltaic performance of the DSC is very remarkable since the efficiency of conventional p–n junction solar cells drops significantly over the same temperature range, reducing performance under real outdoor conditions compared to the standard measuring conditions. Conventional silicon solar cells with efficiency¹¹ of 12–14% suffer a 15–20% loss in initial efficiency over the same temperature range, narrowing their performance advantage over the DSC under realistic outdoor operating conditions.

DSC devices based on the new ionic liquid electrolyte were subjected to long-term stability tests that involved heating at 80 °C in dark and light soaking at 60 °C for 1000 h. Figure 3a shows detailed evaluation of the device parameters during the aging at 80 °C in dark and measured at room temperature. Before measurement, the cell was illuminated under visible light (AM 1.5) for a few hours. During the thermal aging, there was a drop of 1 mA cm⁻² in the short-circuit current density and 40–50 mV in the open-circuit voltage. During this time period, a 5% increase in the FF helped to retain 90% of the initial overall photovoltaic efficiency. This is the first time such an excellent thermal stability at 80 °C was obtained with an ionic liquid electrolyte, which will foster scientific research and industrial applications of flexible DSC devices where ionic liquid electrolytes are preferred.

Electrochemical impedance spectroscopy (EIS) was performed to investigate the interface variation in DSC in order to probe the photovoltaic parameter variations during the aging processes of DSC.¹² Figure 3b,c shows the Bode phase diagrams and Nyquist plots of the DSC device measured in dark at -0.70 V bias before and after the aging at 80 °C for 1000 h. Upon aging, the middle-frequency peak position slightly shifts to higher frequency (Figure 3b), revealing a decrease in the electron recombination time (τ) from 17.1 to 8.9 ms. The decrease of electron lifetime explains the drop of V_{oc} observed upon aging the cells.

Using the equation $D = L^2/\tau_d$, one derives from the fitted τ_d of the lower frequency arc in Figure 3b and the estimated electrolyte layer thickness ($L =$ half of the thickness of the cell)¹³ a diffusion coefficient of triiodide of 6.6×10^{-7} cm² s⁻¹, in agreement with the value determined above by microelectrode voltammetry. The increase in the radius of the low frequency semicircle in the Nyquist plot shows that the diffusion resistance augments during aging probably due to a decrease in the triiodide concentration caused by reaction with impurities.^{11b} The position of the high frequency peak corresponding to the charge transfer reaction at the counter electrode ($I_3^- + 2e = 3I^-$) retains a similar value for fresh and aged cells, indicating a stable interface of Pt/electrolyte.

The DSC device also exhibited photostability when submitted to accelerated testing in a solar simulator at 100 mW cm⁻². The cells were covered with a 50 μ m thick layer of polyester film as a UV cutoff filter (up to 400 nm). The device photovoltaic conversion efficiency retained more than 90% of its initial value even after 1000 h under light soaking at 60 °C (Figure S5).

In conclusion, we have obtained 7.0% energy conversion efficiency at full sunlight by employing a novel ionic liquid, and a stable DSC device performance after aging at 80 °C and under AM 1.5 full sunlight at 60 °C for 1000 h has been demonstrated. Contrary to conventional silicon solar cells, DSC device performances were only negligibly influenced when increasing the operational temperature from ambient to 60 °C. The observed stable performance of IL-based DSCs under accelerated thermal stress and light soaking will further stimulate the practical applications of DSC, particularly in flexible devices.

Acknowledgment. We thank Dr. Qing Wang for his help with the impedance analysis, and P. Comte for the fabrication of TiO₂ paste, Dr. T. Koyanagi (CCIC, Japan) and Dr. Urs Welz-Biermann (Merck AG, Germany) for a free sample of the 400 nm sized light scattering TiO₂ particles and EMIB(CN)₄ ionic liquid, respectively. The Swiss Science Foundation, The Swiss Federal Office for Energy (OFEN) has supported this work.

Supporting Information Available: Molecular structure of EMIB(CN)₄, steady-state voltammogram of binary IL electrolyte, I – V and photocurrent transient curves of DSC measured at different temperature, and light soaking stability (60 °C) data. This material is available free of charge via the Internet at <http://pubs.acs.org>.

References

- O'Regan, B.; Grätzel, M. *Nature* **1991**, *353*, 737.
- Hagfeldt, A.; Grätzel, M. *Chem. Rev.* **1995**, *95*, 40.
- (a) Grätzel, M. *Chem. Lett.* **2005**, *34*, 8–13. (b) Grätzel, M. *Nature* **2001**, *414*, 338.
- (a) Wang, P.; Klein, C.; Humphry-Baker, R.; Zakeeruddin, S. M.; Grätzel, M. *Appl. Phys. Lett.* **2005**, *86*, 123508. (b) Kato, T.; Okazaki, A.; Hayase, S. *Chem. Commun.* **2005**, 363. (c) Kuang, D.; Klein, C.; Snath, H. J.; Moser, J.-E.; Humphry-Baker, R.; Comte, P.; Zakeeruddin, S. M.; Grätzel, M. *Nano Lett.* **2006**, *6*, 769.
- (a) Wasserscheid, P.; Welton, T. *Ionic Liquids in Synthesis*; Wiley: Weinheim, Germany, 2002. (b) Dogers, R. D.; Seddon, K. R. *Science* **2003**, *302*, 792.
- (a) Dupont, J.; de Souza, R. F.; Suarez, P. A. Z. *Chem. Rev.* **2002**, *102*, 3667. (b) Xu, W.; Angell, C. A. *Science* **2003**, *302*, 422.
- (a) Kubo, W.; Kitamura, T.; Hanabusa, K.; Wada, Y.; Yanagida, S. *Chem. Commun.* **2002**, 374. (b) Wang, P.; Zakeeruddin, S. M.; Moser, J. E.; Grätzel, M. *J. Phys. Chem. B* **2003**, *107*, 13280. (c) Wang, P.; Zakeeruddin, S. M.; Humphry-Baker, R.; Grätzel, M. *Chem. Mater.* **2004**, *16*, 2694. (d) Wang, P.; Wenger, B.; Humphry-Baker, R.; Moser, J. E.; Teuscher, J.; Kantelechner, W.; Mezger, J.; Stoyanov, E. V.; Zakeeruddin, S. M.; Grätzel, M. *J. Am. Chem. Soc.* **2005**, *127*, 6850. (e) Kuang, D.; Ito, S.; Wenger, B.; Klein, C.; Moser, J.-E.; Humphry-Baker, R.; Zakeeruddin, S. M.; Grätzel, M. *J. Am. Chem. Soc.* **2006**, *128*, 4146.
- (a) Bernhardt, E.; Henkel, G.; Willner, H. *Z. Allg. Anorg. Chem.* **2000**, *626*, 560. (b) Brnhardt, E.; Finze, M.; Willner, H. *Z. Allg. Anorg. Chem.* **2003**, *629*, 1229.
- Welz-Biermann, U.; Ignatyev, N.; Bernhardt, E.; Finze, M.; Willner, H. (Merck GmbH, Darmstadt, Germany) Patent WO 2004/072089 A1, 2004.
- Bard, A. J.; Faulkner, L. R. *Electrochemical Methods: Fundamentals and Applications*, 2nd ed.; Wiley: Weinheim, Germany, 2001.
- Efficiency of close to 24% has been reached with single-crystal Si champion laboratory cells.
- (a) Bisquert, J. *J. Phys. Chem. B* **2002**, *106*, 325. (b) Wang, Q.; Moser, J. E.; Grätzel, M. *J. Phys. Chem. B* **2005**, *109*, 14945.
- Hauch, A.; Georg, A.; Baumgärtner, S.; Opar-Krasovec, U.; Orel, B. *Electrochim. Acta* **2001**, *46*, 2131.

JA061714Y